JOURNAL OF THERMOPHYSICS AND HEAT TRANSFER
Vol. 23, No. 2, April–June 2009

Effect of the Coolant Ejection in Rectangular and Trapezoidal Trailing-Edge Cooling Passages

Lesley M. Wright*
Baylor University, Waco, Texas 76798-7356
and
Amir S. Gohardani†
University of Arizona, Tucson, Arizona 85721-0119

DOI: 10.2514/1.38426

Heat transfer coefficients are experimentally determined in various trailing-edge cooling channels. A rectangular channel (AR = 3:1) with fully developed flow is used as a baseline for the study, with the Reynolds number varying from 20,000 to 80,000. The heat transfer coefficients in this channel are compared with those in a similar rectangular channel with coolant extraction, which would likely be encountered in a trailing-edge cooling passage. The heat transfer trends in the rectangular channel are compared with those obtained in a passage with a trapezoidal (or wedge-shaped) cross section. The heat transfer coefficients are also obtained in the channel without coolant extraction and with extraction from the narrow side of the channel. The effect of V-shaped rib turbulators is also considered in the rectangular and trapezoidal cooling passages. In addition, the effect of entrance condition is considered with the wedge-shaped channel. Heat transfer coefficients obtained with hydrodynamically developed flow are compared with those with flow through a contraction into the heated section of the channel. In the rectangular channel without ejection, the heat transfer coefficients are uniform across the span of the channel; however, with coolant ejection, the heat transfer coefficients increase near the ejection slots. In addition, in the trapezoidal channels, the heat transfer coefficients are uniform across the cross section of the smooth channel. When coolant is extracted for trailing-edge ejection, the outer surface sees the most significant heat transfer enhancement. The outer surface of the smooth trapezoidal channel is most profoundly affected by the entrance condition, and the effect of the entrance condition is marginal in trapezoidal channels with ribs and ejection.

Nomenclature

A	=	surface area of the copper plate, cm^2
AR	=	channel aspect ratio, W/H
c_p	=	specific heat of the coolant, kJ/kg · K
D_h	=	hydraulic diameter, cm
e	=	rib height, cm
H	=	channel height, cm
h	=	heat transfer coefficient, W/m^2 · K
k	=	thermal conductivity of the coolant, W/m · K
L	=	heated length of the duct, cm
$\dot{m}$	=	mass flow rate of the coolant, kg/s
$\dot{m}_j$	=	mass flow rate of the coolant through ejection, given the ejection slot, kg/s
$\dot{m}_n$	=	local mass flow rate of the coolant at x location, kg/s
Nu	=	regionally averaged Nusselt number, hD_h/k
Nu_o	=	Nusselt number for flow in a fully developed, turbulent, nonrotating smooth tube
P	=	rib pitch, cm
P_{exit}	=	exit pressure for a trailing-edge ejection slot, kPa
P_{in}	=	inlet pressure for a trailing-edge ejection slot, kPa
Pr	=	Prandtl number
Q	=	rate of heat transfer, W
Q_{net}	=	net rate of heat transfer, W
q''_{net}	=	net heat flux at wall, W/m^2
Re_{in}	=	Reynolds number, $\rho V_{\text{in}} D_h/\mu$
Re_x	=	local Reynolds number
$T_{b,i}$	=	bulk coolant temperature at the channel inlet, °C
$T_{b,x}$	=	regional coolant temperature, °C
$T_{w,x}$	=	regional wall temperature, °C
V_{in}	=	bulk velocity in streamwise direction at the channel inlet, m/s
W	=	channel width, cm
x	=	streamwise location, cm
α	=	rib angle
ρ	=	fluid density, kg/m^3

Received 6 May 2008; revision received 28 October 2008; accepted for publication 3 November 2008.

*Department of Mechanical Engineering; Lesley_Wright@Baylor.edu. Member AIAA.
†Department of Aerospace and Mechanical Engineering.

Introduction

GAS turbines play a vital role in today's industrialized society, and as the demands for power increase, the power output and thermal efficiency of gas turbines must also increase. One method of increasing both the power output and thermal efficiency of the engine is to increase the temperature of the gas entering the turbine. In the advanced gas turbines of today, the turbine inlet temperature can be as high as 1500°C; however, this temperature exceeds the melting temperature of the metal airfoils. Therefore, it is imperative that the blades and vanes are cooled so that they can withstand these extreme temperatures. Cooling air around 600°C is extracted from the compressor and passes through the airfoils. With the hot gases and cooling air, the temperature of the blades can be lowered to approximately 1000°C, which is permissible for reliable operation of the engine.

Designers need new internal heat transfer data to improve current blade and vane cooling performances. They also need detailed flow and heat transfer data to understand the flow physics and to improve the current internal cooling designs. These data will also aid in the validation of new computational fluid dynamics codes to more accurately model the airfoil cooling passages. Many techniques have been developed to enhance the heat transfer in these passages. The cooling passages located in the middle of the airfoils are often lined with rib turbulators. Near the leading edge of the blade, jet impingement (coupled with film cooling) is commonly used. Jet impingement is also used throughout the cross section of the stator

vanes. Pin fins and dimples can be used in the trailing-edge portions of the vanes and blades. These techniques have also been combined to further increase the heat transfer from the airfoil walls. A number of traditional cooling concepts are used in various combinations to adequately cool the turbine vanes and blades. Han et al. [1] provide a more in-depth description of turbine-blade heat transfer and cooling technology for the interested reader.

Han et al. [1] compiled a comprehensive review of gas turbine cooling technology, including many techniques to enhance the heat transfer within the internal cooling passages. They include numerous studies that have been conducted over the years on a wide range of rib configurations in various-sized cooling channels using many experimental techniques. Early studies investigated cooling channels with orthogonal ribs (Han [2]). It was then determined that placing the ribs at an angle to the mainstream flow will result in greater heat transfer enhancement than with the ribs positioned at 90 deg to the mainstream flow. Studies by Han and Park [3] and Park et al. [4] investigated the thermal performance of angled ribs compared with orthogonal ribs. The results showed that the heat transfer enhancement in angled-rib channels is significantly greater than the heat transfer enhancement due to normal ribs.

The focus of rib turbulators began to shift to the investigation of high-performance ribs. Han et al. [5] studied a square channel with V-shaped, L-shaped, parallel (angled), and crossed ribs. They showed that the V-shaped ribs (45 and 60 deg) perform better than the parallel ribs (45 and 60 deg). Using the mass transfer technique, Lau et al. [6] found that the V-shaped ribs create the greatest heat transfer enhancement; however, they also create the greatest pressure drop. Their results showed that the V-shaped ribs and the full (angled) ribs had comparable thermal performances. Han and Zhang [7] then completed a study of a square channel with various angled and V-shaped rib configurations. They concluded that broken ribs (similar to discrete ribs) create heat transfer enhancement levels of 2.5–4, whereas the enhancement created by the continuous ribs is only 2–3. Both the broken and continuous ribs incur a pressure penalty of 7–8 times that of a smooth channel. Taslim et al. [8] studied various configurations of angled and V-shaped ribs using a liquid-crystal technique. They also concluded that V-shaped ribs result in the greatest heat transfer enhancement and have the greatest pressure loss. Ekkad and Han [9] also used a liquid-crystal technique to obtain detailed heat transfer distributions in a two-pass channel with parallel (angled), V-shaped, and broken V-shaped (discrete V-shaped) ribs. They concluded that the parallel, V-shaped, and broken V-shaped ribs produce similar heat transfer enhancement in the first pass, with the broken V-shaped ribs giving slightly higher enhancement.

Cho et al. [10] recently investigated angled and discrete angled ribs using mass transfer. They concluded that the heat transfer performance of the discrete ribs is similar to that of the angled ribs in a rectangular channel with an aspect ratio of 2.04:1. A very narrow channel ($AR = 8{:}1$) with V-shaped, L-shaped, and angled ribs was studied by Gao and Suden [11]. Using a liquid-crystal technique, they too confirmed that V-shaped ribs result in the highest heat transfer enhancement and the highest frictional losses. They concluded that the V-shaped ribs yield the best overall thermal performance. Rhee et al. [12] also investigated rectangular channels ($AR = 3{:}1, 5{:}1$, and $6.82{:}1$). They studied the thermal performance of V-shaped and discrete V-shaped ribs. Based on their configurations, they concluded that the thermal performance of the two configurations were comparable.

The study of internal turbine-blade heat transfer should not be limited to square and rectangular channels. As previous studies have shown, the cross-sectional area of the cooling channel has a profound effect on the heat transfer enhancement within the channel. The cooling channels may have cross sections that are not square or rectangular, the channels near the leading edge may have a triangular cross section, and channels near the trailing edge may be triangular or trapezoidal, as shown in Fig. 1.

Heat transfer coefficients have been measured in a variety of triangular cooling channels. The heat transfer and friction coefficients measured in smooth equilateral triangles are in good agreement with the established correlations developed for tube flow,

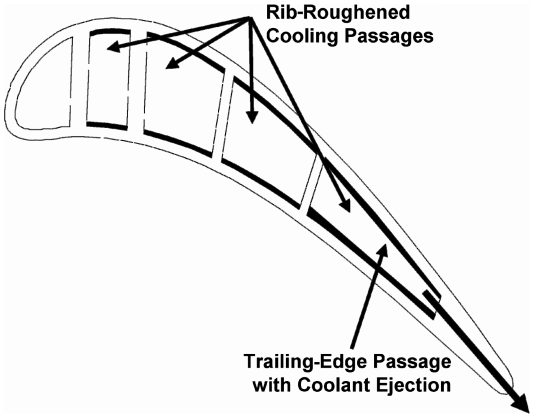

Fig. 1 Typical cross section of a cooled turbine blade.

with the hydraulic diameter of the triangular duct replacing the tube diameter [13,14]. When the cross section of the channel changes from an equilateral triangle to a scalene triangle, similar conclusions have been drawn. Obot [15] concluded that the heat transfer coefficients measured in the fully developed region of a scalene triangular duct are comparable with those predicted by the established Colburn equation for fully developed turbulent flow through a smooth tube. Similar conclusions were drawn by Zhang et al. [16] with their right-triangle duct; in their channel with smooth walls, the heat transfer coefficients were adequately predicted with the McAdams correlation, and the friction factors could be estimated with the Blasius equation for turbulent flow through smooth tubes.

Initially, it would appear that heat transfer and friction coefficients can be estimated using well-known correlations developed for circular tubes. However, further experimental investigations have produced contrary conclusions. Eckert and Irvine [17] measured the friction and heat transfer coefficients in an isosceles triangle channel with an apex angle of 11.5 deg. With this relatively small apex angle, they concluded that the friction factors for this channel were lower than those predicted from correlations. They also showed significant deviation of the heat transfer coefficients compared with those predicted by established correlations. This study also showed that the thermal entrance length for their duct was greater than 100 hydraulic diameters (compared with an entry length of 10 to 20 diameters for circular tubes).

To more closely model trailing-edge cooling channels, it is important to consider how the heat transfer trends are affected as the coolant is extracted from the channels for trailing-edge film cooling. Lau et al. [18,19] and Kumanran et al. [20] measured the heat transfer and friction in rectangular channels with trailing-edge ejection. In these rectangular channels with pin fins, they concluded that the heat transfer coefficients through the channel drop with the addition of trailing-edge ejection. This should be expected, as the flow rate of the coolant decreases in the streamwise flow direction. Taslim et al. [21] used a more realistic trapezoidal (wedge-shaped) channel with trailing-edge ejection. They showed that in a smooth wedge-shaped channel, the average heat transfer coefficients were adequately predicted with the Dittus-Boelter correlation. They also showed that significant spanwise variation is present in this channel. However, when trailing-edge ejection is introduced, this spanwise variation is reduced due to the lateral flow. Hwang and Lu [22] also studied the effect of trailing-edge ejection in trapezoidal ducts. They confirmed that the fully developed heat transfer coefficients in the trapezoidal duct (without bleed flow) are comparable with those predicted by the Dittus-Boelter correlation. They also concluded that increasing the ejection rate increases the heat transfer coefficients on the narrow side of the channel at the cost of reducing the heat transfer coefficients on the wide side of the channel.

Because channel flow has a wide variety of applications, many groups have experimentally investigated the heat transfer enhancement in a wide variety of cooling channels. Square and rectangular channels have been considered extensively, and additional work has been completed on other cross sections (i.e., triangular and

trapezoidal). Contradictory results have been reported for triangular and trapezoidal cooling channels. The trends in equilateral triangles are similar to those in square and circular tubes. However, the trends in triangular channels with small apex angles vary dramatically from circular tubes, and the trends in trapezoidal channels can be predicted from smooth-tube correlations. The current experimental study will consider both rectangular and trapezoidal (wedge-shaped) channels to help bridge the gap between these two cross sections. Heat transfer coefficients will be measured in rectangular channels with smooth and rib-roughened walls. The effect of trailing-edge ejection will be considered in these rectangular channels. A wedge-shaped channel that more appropriately models a trailing-edge cooling channel will also be considered. Both smooth and rib-roughened trapezoidal channels will be considered to evaluate the effect of channel cross section. The effect of the coolant extraction will be considered along with the effect of channel entrance condition (simultaneous development of the hydrodynamic and thermal boundary layers).

Experimental Facilities

Facility Overview

The heat transfer experiments were performed using a large-scale channel to model a typical internal cooling passage located near the trailing edge of the turbine blade or vane. A 7.5 hp motor powers a blower that supplies cooling air to the channel. The mass flow rate through the system is set by adjusting a variable-frequency-drive controller attached to the motor.

The test section is a one-pass channel with a rectangular aspect ratio of 3:1. As shown in Fig. 2, the cooling air first travels through an unheated entrance section before entering the heated portion of the test section. As shown in the figure, the entrance is 47 cm long, and the cross section of this region can be varied. By varying the entrance geometry, the effect of flow development on the heat transfer enhancement can be independently considered. Wire screens are placed in this entrance region to assist in uniforming the flow. The heated portion of the test section is 38.1 cm long, with a 5.08 cm unheated section at the end of the channel.

Only two walls of the test section are heated: one wide wall and one narrow wall. These surfaces are fabricated of grade G-11 garolite (whereas all other surfaces are fabricated from polycarbonate). The wide surface is divided into three regions, to provide an adequate spanwise distribution in the heat transfer coefficients. In addition, the narrow wall (opposite of the trailing-edge ejection) is instrumented. Each spanwise region is equipped with an electric heater supplying a uniform heat flux. Therefore, a total of four heaters are used: one for the narrow wall, one for the inner region, one for the middle region, and one for the outer region. Figure 3 shows the surface designations for the present investigation. Streamwise heat-transfer-coefficient distributions are obtained with 15 individual copper plates aligned in the flow direction. With the 4 spanwise regions and the 15 streamwise regions, a total of 60 regional measurements can be obtained.

With one heater used for each spanwise region (15 regions in the streamwise direction), the thermal boundary condition of the channel is neither constant heat flux nor constant wall temperature; it is actually a combination of the two. In the streamwise direction, constant heat flux is applied to each region, whereas circumferentially, the four regions are maintained at approximately the same temperature (with a temperature distribution in the streamwise direction). This thermal boundary condition (combined with two unheated walls) is not an exact representation of thermal boundary conditions encountered within the engine. However, for this stationary channel, this should not distract the reader, as the heat transfer coefficients are relatively insensitive to the boundary condition in highly turbulent flows. The thermal boundary condition gains importance in rotating channels, in which the rotational buoyancy force has a significant impact on the heat transfer enhancement within the channel.

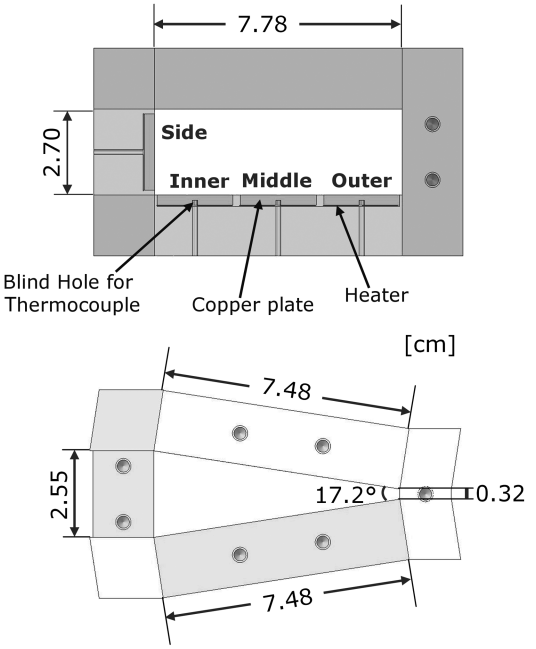

Fig. 3 Cross-sectional view of the rectangular and trapezoidal channels.

The copper plates used for regional measurements are $2.38 \times 2.38 \times 0.318$ thick. Surrounding each copper plate is a 0.159 cm silicone insulating strip. This layer of insulation minimizes conduction between two adjacent copper plates. To maintain approximately the same circumferential wall temperature, the power supplied to the heaters is varied. Although maintaining the same temperature at two adjacent copper plates, the net heat flux can vary by 72% (the extreme case involving V-shaped ribs and ejection). Therefore, the nylon strip is effectively limiting the conduction between adjacent copper plates.

A blind hole is drilled in the back of each copper plate, and a thermocouple is secured in the blind hole approximately 0.159 cm from the surface of the copper plate. The type-T thermocouples are secured with high-conductivity thermal epoxy. The thermocouple output is monitored using commercially available software. The temperature data are displayed using the virtual instrument format, and the data are written to a data file specified by the user. The resistance heaters are placed beneath the copper plates, and thermal paste is used to reduce the contact resistance between the copper and the heater. The four heaters are connected to four variable transformers so that the wall heat flux is varied to maintain temperature uniformity circumferentially. The entire test section is wrapped in insulation to reduce heat loss from the test section.

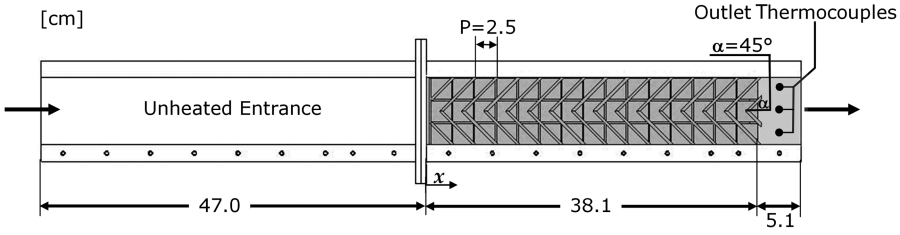

Fig. 2 Test-section details (unheated entrance and heated test section); shown with V-shaped ribs.

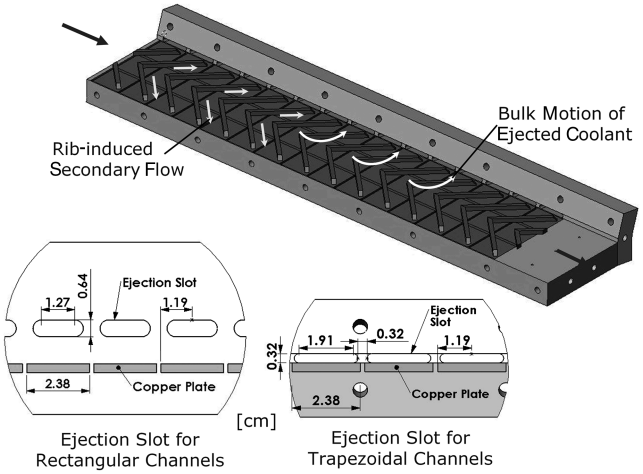

Fig. 4 Details of the trailing-edge ejection slots.

Static-pressure taps are used to measure the pressure distribution through the heated portion of the test section. The pressure taps are located on the wide surface, opposite to the heated wall. A 16-channel Scanivalve pressure transducer is used to measure the static pressure at each of the taps. The pressure measurements are taken under adiabatic conditions (test section is not heated).

Trailing-Edge Configurations

This experimental investigation evaluates a total of 12 channel configurations. The configurations include variable channel cross section, surface roughness, entrance condition, and trailing-edge extraction. The baseline case consists of a 3:1 rectangular channel with smooth walls. As shown in Fig. 3, the channel is 7.78×2.70 cm (the resulting hydraulic diameter is 4.0 cm), with the unheated entrance being 12 hydraulic diameters long. Heat-transfer-coefficient distributions are obtained in this channel with and without trailing-edge extraction. When the effect of extraction is considered, all of the cooling air is forced through the ejection slots, as the end of the channel is completely blocked. For the rectangular channel, 15 ejection slots line the channel, and the cross section of each slot is shown in Fig. 4. To more adequately model a cooling passage, the heated wide wall of the channel is lined with rib turbulators. Square ribs with a cross section of 0.318×0.318 cm are used. As shown in Fig. 2, the ribs are arranged in a V-shaped pattern. The pitch-to-height ratio is 8, and the height-to-hydraulic-diameter ratio is 0.079. The ribs are oriented at 45 deg to the mainstream flow.

In the narrow trailing-edge region of the blades, the cooling channels are more likely to have a wedge-shaped cross section. The wedge shape is also modeled as shown in Fig. 3. The wedge, or trapezoidal, channel has a hydraulic diameter of 2.38 cm (the unheated entrance approaches 20 hydraulic diameters in length). The heated narrow wall remains unaltered, but the opposite narrow wall is reduced to 0.318 cm in height. As with the rectangular channel, the effect of the coolant extraction is considered with the addition of the cooling slots on the narrow wall. Because of space limitations, the ejection slot varies slightly from that used with the rectangular channel, and the dimensions of the slot are shown in Fig. 4. The effect of surface roughness is also investigated. As with the rectangular channel, square ribs (0.318×0.318 cm) are used in a V pattern. Although the pitch-to-rib-height ratio remains at 8, the rib-height-to-hydraulic-diameter ratio increases to 0.133 (due to the reduced hydraulic diameter). In addition, the length of the ribs is reduced to allow clearance on the narrow side of the channel.

Because flow is rarely hydrodynamically developed when it enters the turbine blade, the effect of developing flow is also considered in this study. The effect of a sharp entrance (sudden contraction) is studied by coupling the rectangular entrance duct with the heated trapezoidal test section (this is only one possible entrance condition that might be encountered in the airfoil cooling passage). With a rectangular entrance feeding a trapezoidal test channel, the contraction ratio varies across the channel. From the wide (inner) side to the narrow (outer) side of the channel, the contraction ratio varies from 1:1 to 8.5:1. Therefore, the outer surface is affected more by the entrance condition than are the inner and side surfaces. Table 1 summarizes the 12 cases considered in this study.

Data Reduction

This study investigates the regionally averaged heat transfer coefficient at various locations within the trailing-edge cooling channels. The heat transfer coefficient is determined by the net heat transferred from the heated plate, the surface area of the plate, the regionally averaged temperature of the plate, and the local bulk mean temperature in the channel. Therefore, the heat transfer coefficient is given as

$$h = \frac{Q_{\text{net}}/A}{T_{w,x} - T_{b,x}} \tag{1}$$

The net heat transfer is calculated using the measured voltage and current supplied to each heater from the variable transformers multiplied by the area fraction of the heater exposed to the respective plate minus the external heat losses escaping from the test section. The heat losses are predetermined by performing a heat loss calibration. The heat loss calibration is performed by inserting insulation into the channel to eliminate natural convection. During the calibration, the heat transfer (in the form of power from the variable transformers) and regional wall temperature of each plate is measured; therefore, from the conservation-of-energy principle, it is possible to know how much heat is being lost to the environment. The heat loss calibration is repeated for each channel configuration, and so a local heat loss distribution is obtained for each channel considered in study. At a Reynolds number of 20,000, heat losses account for 17% of the heat put into the test section. However, at a higher Reynolds number of 80,000, just less than 6% of the heat input is lost by conduction through the test section.

The surface area used in this study is the projected surface area of the channel: in other words, the surface area of a smooth channel (the area increase due to the ribs is neglected). Although the V-shaped

Table 1 Experimental-case summary

Case number	Channel cross section	Trailing-edge ejection	Wall roughness	Entrance condition
1	Rectangular	No	Smooth	Fully developed
2	Rectangular	Yes	Smooth	Fully developed
3	Rectangular	No	V-shaped ribs	Fully developed
4	Rectangular	Yes	V-shaped ribs	Fully developed
5	Wedge	No	Smooth	Fully developed
6	Wedge	Yes	Smooth	Fully developed
7	Wedge	No	Smooth	Contraction
8	Wedge	Yes	Smooth	Contraction
9	Wedge	No	V-shaped ribs	Fully developed
10	Wedge	Yes	V-shaped ribs	Fully developed
11	Wedge	No	V-shaped ribs	Contraction
12	Wedge	Yes	V-shaped ribs	Contraction

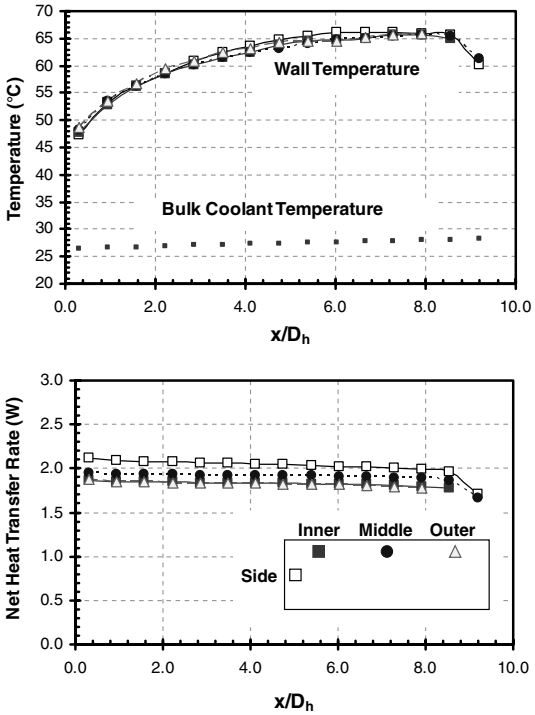

Fig. 5 Typical wall- and coolant-temperature distributions.

ribs increase the heat transfer by approximately 29%, this area is neglected to provide a fair assessment of the heat transfer enhancement within the channel. The regionally averaged wall temperature T_w is directly measured using the thermocouple installed in the blind hole on the backside of each copper plate. Because the plates are made of the copper, which has a high thermal conductivity, the temperature of each plate is assumed to be uniform. One thermocouple at the inlet and three thermocouples at the outlet of the test section measure the inlet and outlet bulk temperatures, respectively. The local bulk temperature is calculated using the conservation-of-energy principle. The energy balance equation is

$$T_{b,x} = T_{b,i} + \sum_i \frac{(Q - Q_{\text{loss}})}{\dot{m} c_p} \qquad x = 1, 2, \ldots, 15 \tag{2}$$

All air properties are taken based on the bulk air temperature with a Prandtl number Pr for air of 0.71. Figure 5 shows the wall-temperature and coolant-temperature distributions of a typical test. Also shown in this figure is the heat rate distribution (both spanwise and streamwise). As discussed previously, a mixed thermal boundary condition is employed, and this is represented by the streamwise uniformity of the net rate of heat transfer and the spanwise variation (minimal for the smooth rectangular channel that is presented).

When trailing-edge ejection is considered, the local mass flow rate decreases in the streamwise direction. To make fair comparisons, it is necessary to know how the Reynolds number varies through the channel. The mass flow rate through any ejection slot can be estimated using Eq. (3) (from Kumaran et al. [20]):

$$\dot{m}_j = C_D A_j \sqrt{2^* \rho^* (P_{\text{in}} - P_{\text{exit}})} \tag{3}$$

where C_D is the discharge coefficient, and Aj is the cross-sectional area of the slot. The density is obtained by the pressure and bulk temperature at each location. The pressure inside the channel at each location is measured through the static-pressure taps located through the channel. The coolant discharges into the room; therefore, the P_{exit} is taken as ambient pressure. When trailing-edge ejection is considered, the end of the channel is blocked. Therefore, all of the coolant entering the channel must exit through the ejection slots. In other words, the sum of the mass flow rate through the 15 ejection slots must equal the mass flow rate into the channel.

Following the procedure of Kumaran et al. [20], the discharge coefficient is assumed to be constant for all 15 slots. With this assumption, a mass flow rate ratio can be calculated for each segment within the channel:

$$\frac{\dot{m}_n}{\dot{m}} = 1 - \frac{\sum_{n=1}^{n-1} \dot{m}_j}{\dot{m}} \tag{4}$$

There are a total of 15 regions in the streamwise direction within the channel. The local mass flow rate in each region of the channel is the average of the radially inlet and radially outlet mass flow in that region, as shown in Eq. (5):

$$\frac{\dot{m}_{xn}}{\dot{m}} = \frac{\dot{m}_{n-1} + \dot{m}_n}{2\dot{m}} \tag{5}$$

The experimental uncertainty for the presented results was calculated using the method developed and published by Kline and McClintock [23]. The estimated uncertainty in the temperature measurements is 0.5°C for all cases. At the Reynolds number of 20,000, the overall uncertainty in the Nusselt number ratio is approximately 13% of the presented values. At the lowest Reynolds number, a greater percentage of the heat input is lost. Because of the estimation of these heat losses, the experimental uncertainty increases. However, at the higher Reynolds numbers, the percent uncertainty of the individual measurements decreases and the percentage of heat losses decreases. Therefore, the overall uncertainty in the Nusselt number ratio decreases to approximately 5% of the calculated value at a higher Reynolds number of 80,000.

Results and Discussion

Rectangular Cooling Passages

The presentation of the results begins with an evaluation of the current experimental setup. To validate the use of the experimental facility, heat transfer coefficients are obtained in the smooth rectangular channel (case 1). The flow is hydrodynamically developed when it enters the heated portion of the test section, and the walls within the heated section are smooth. The heat transfer coefficients are presented in the form of the nondimensional Nusselt number. These Nusselt numbers are compared with the accepted value as predicted by the Dittus-Boelter/McAdams correlation [24] and shown in Eq. (6):

$$\frac{Nu}{Nu_o} = \frac{hD_h}{k} \frac{1}{0.023 Re^{0.8} \text{Pr}^{0.4}} \tag{6}$$

Figure 6 shows the Nusselt number ratios for case 1. For all four Reynolds numbers shown, the Nusselt number ratios follow the same trends. Heat transfer enhancement is observed near the inlet of the test section. These elevated heat transfer coefficients result from the development of the thermal boundary layer that forms at the inlet of the heated test section. The Nusselt number ratios decrease to a constant value of 1 at approximately 6 diameters into the channel. This behavior is observed for all four heated regions, and this behavior is expected for a channel with the prescribed thermal boundary conditions. Therefore, it can be concluded that the channel is sufficient long to establish by hydrodynamically and thermally developed flow.

With the experimental setup yielding reliable results, it is possible to move on to more realistic cooling configurations. The effect of trailing-edge ejection is considered with case 2. Before viewing the heat-transfer-coefficient distributions, it is necessary to investigate how the Reynolds number varies through the channel. Figure 7 shows the local Reynolds number variation for case 2. As shown in the figure, the Reynolds number decreases in the flow direction, due to the coolant extraction. The Reynolds number approaches zero near the end of the channel, as 100% of the coolant is forced through the ejection slots. With knowledge of the flow behavior through the channel, heat-transfer-coefficient distributions can be considered. Figure 8 shows the regionally averaged Nusselt numbers for a smooth rectangular channel with trailing-edge ejection (case 2). On

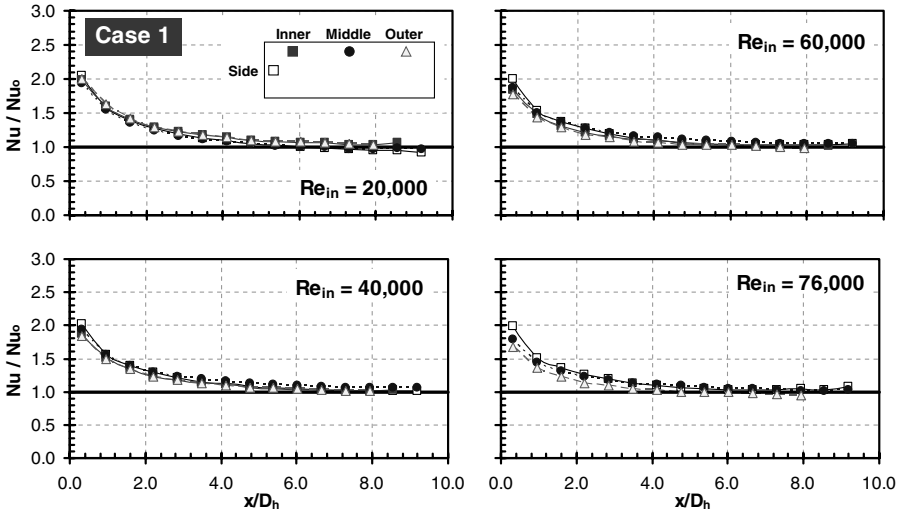

Fig. 6 Nusselt number ratios for case 1.

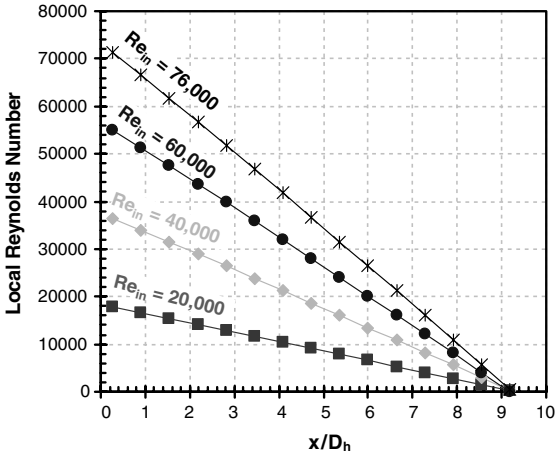

Fig. 7 Local Reynolds number distribution for case 2.

each plot, the fully developed Nusselt number as predicted by the Dittus-Boelter/McAdams correlation for the inlet Reynolds number is shown in black. The general trends for each surface and Reynolds number follow those of case 1: a gradual decrease in the heat transfer coefficients from the entrance of the test section. For all four flow rates tested, the Nusselt numbers fall below those predicted by the correlation within the first half of the channel.

As x/D_h increases for case 2, the variation of the heat transfer coefficients on each surface increases. Near the entrance of the channel, all four surfaces experience the same level of heat transfer enhancement. However, as coolant is expelled from the channel, the outer surface experiences increased heat transfer. The coolant accelerates in the lateral direction through the ejection slots, and the outer surface is the beneficiary of increased heat transfer coefficients resulting from the relatively thin thermal boundary layer. As anticipated, the Nusselt numbers are lowest on the inner and side surfaces, as the core of the coolant is pulled away from this area within the channel.

To increase the heat transfer within the internal cooling passages, the passages are typically lined with turbulators. V-shaped rib turbulators were used in the present investigation. Figure 9 shows the heat transfer enhancement in rib-roughened rectangular channels (with and without trailing-edge ejection). The heat transfer enhancement is presented in terms of a Nusselt number ratio for a single mass flow rate ($Re_{\text{in}} = 60,000$). The Nusselt numbers obtained in the case without ejection (case 3) are normalized by the corresponding smooth-channel data (case 1), and case 4 is similarly normalized by the Nusselt number obtained for case 2.

The Nusselt number ratios vary significantly in both the spanwise and streamwise directions for case 3. The heat transfer coefficients gradually increased from a minimum at the entrance of the channel. Others have shown [25,26] that V-shaped ribs induce secondary flow that results in two pairs of counter-rotating vortices forming along the legs of the V. The strength of these vortices increases in the flow

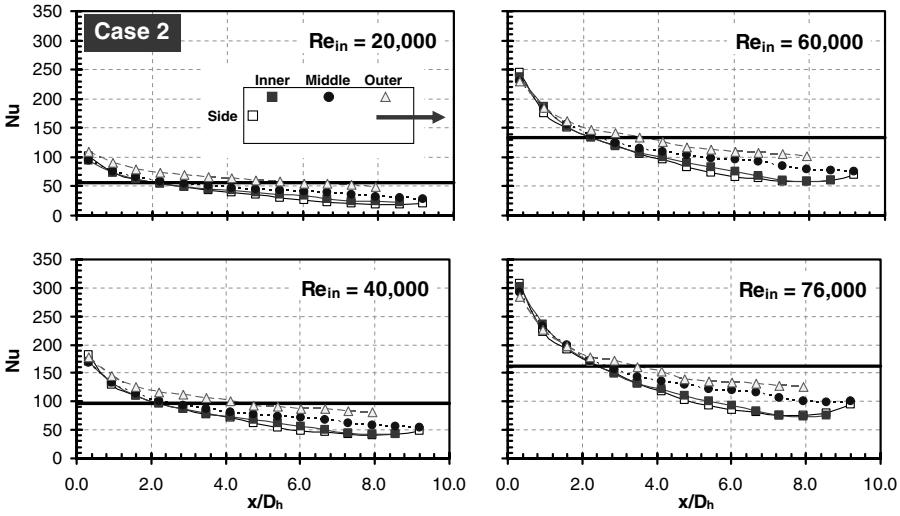

Fig. 8 Nusselt number distributions for case 2.

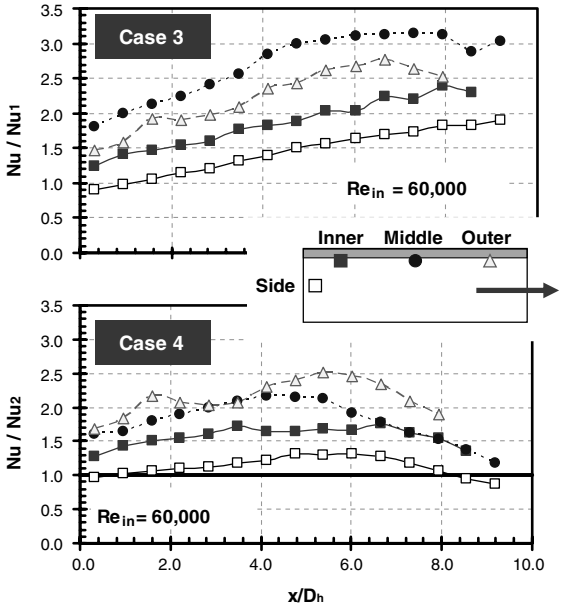

Fig. 9 Nusselt number ratios for cases 3 and 4.

direction through the channel. As the strength of the secondary flow increases, the heat transfer coefficients increase. The middle region obviously experiences the greatest heat transfer enhancement. Near the surface, the secondary flow moves from the center of the channel, along the legs, to the outer walls of the channel. Therefore, the boundary layer forms at the center of the V and grows away from the center of the channel. The center of the channel experiences the greatest heat transfer enhancement, as the boundary layer along the rib is relatively thin and more mixing with the core of the coolant exists. The lowest Nusselt number ratios occur on the side wall. This is expected, as the side wall remains smooth and heat transfer enhancement results from additional mixing of the coolant through the channel.

The inner and outer regions do not experience the same level of heat transfer enhancement. As Fig. 9 shows, the heat transfer coefficients on the outer surface are greater than those on the inner surface. This trend was unexpected, due to the symmetrical layout of the turbulators. However, this variation can be explained by examining the thermal boundary conditions. The outside wall (in contact with the outer surface) is unheated, whereas the opposing side wall is heated. As the secondary flow travels along the turbulator from the center to the side wall, heat is transferred to the coolant. Additional heat is transferred to the coolant from the heated side wall. However, next to the outer surface, the coolant does not gain heat from the outside wall. As the coolant circulates within the rib-induced counter-rotating vortices, the coolant in contact with the outside wall will be cooler than that in contact with the inner wall. The result is increased heat transfer on the outer surface (compared with the inner surface).

The effect of the coolant extraction in a rib-roughened channel can be seen with case 4 in Fig. 9. Unlike case 3, the heat transfer coefficients increase to a maximum before decreasing through the channel. Also, the spanwise variation differs from that observed with case 3. The V-shaped ribs yield increased heat transfer in the center of the channel, whereas trailing-edge ejection increases the heat transfer coefficients on the outer surface. Although case 4 has been normalized with the Nusselt numbers from case 2, the enhancement on the outer surface remains evident. Enhancement on the side surface is marginal (when compared with case 2), and this is anticipated, as the coolant is forced away from this surface regardless of the surface roughness.

Trapezoidal Cooling Passages

Internal cooling passages located near the trailing edges of turbine blades and vanes generally have a nonuniform cross section that closely follows the cross section of the airfoil. Therefore, it is imperative to investigate the heat transfer behavior in channels with cross sections that more readily model a trailing-edge passage. Figure 10 shows the regional Nusselt number ratios for flow through a trapezoidal channel without trailing-edge ejection. As with Fig. 6, the measured Nusselt numbers are compared with those predicted by the Dittus-Boelter/McAdams correlation. Similar to the results for case 1, the Nusselt number ratios for case 5 show only marginal spanwise variation. The streamwise variation is the result of the thermal-boundary-layer development at the entrance of the channel. For the four Reynolds numbers shown, a fully developed Nusselt number ratio is achieved by $x/D_h = 5$. However, the fully developed Nusselt number ratio is not unity; it is actually less than one. This result is in agreement with the findings of Eckert and Irvine [17] for a triangular channel with an apex angle of 11.46 deg. They observed that the heat transfer coefficients can be less than half of those predicted by the Dittus-Boelter/McAdams correlation. Although the current deficit is approximately 25%, this trend has been observed by other groups, and the discrepancy has called into question the use of the hydraulic-diameter definition for such cross sections with narrow apexes.

The effect of trailing-edge ejection in a smooth trapezoidal channel is shown with case 6 in Fig. 11. As with the rectangular channel, the outer surface benefits the greatest from the trailing-edge ejection, whereas variation between the other surfaces is marginal. The Nusselt numbers decrease in the flow direction as the coolant is

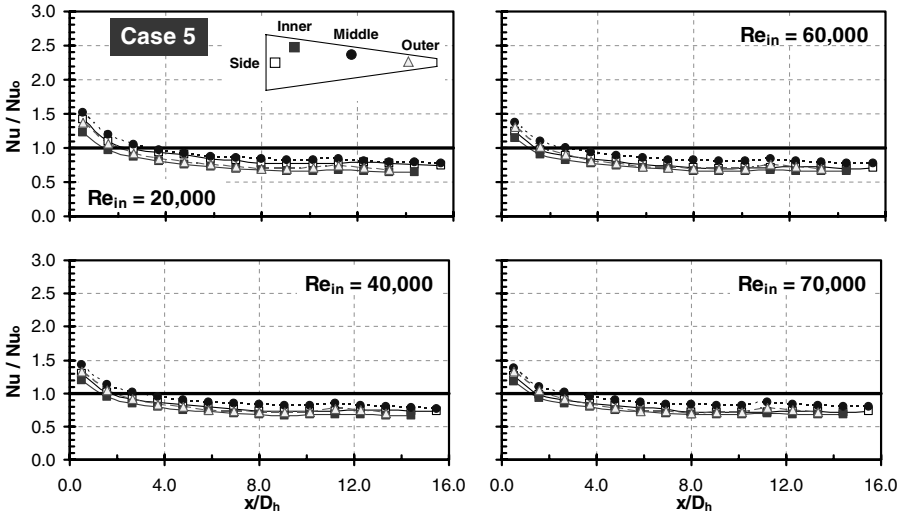

Fig. 10 Nusselt number ratios for case 5.

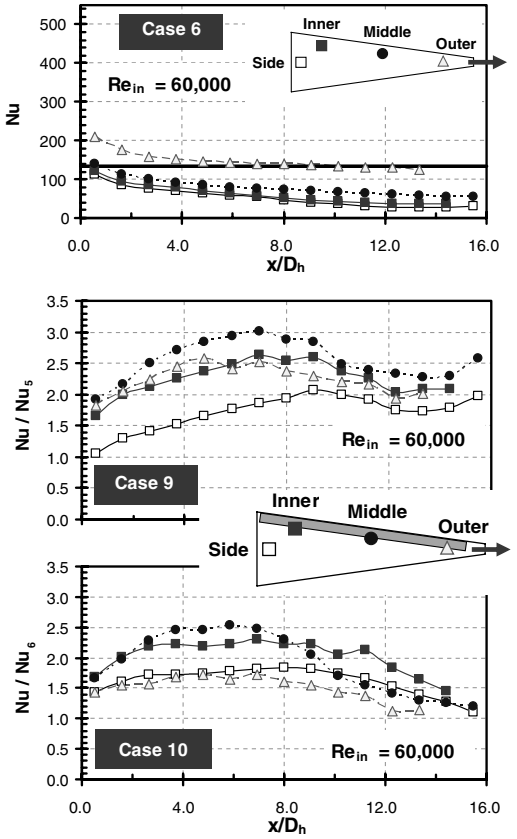

Fig. 11 Nusselt number ratios for cases 6, 9, and 10.

extracted from the channel. Although not shown, similar trends can be observed for other Reynolds numbers that were tested.

The effect of V-shaped ribs placed in the trailing-edge channel is also shown in Fig. 11. With case 9, there is no trailing-edge ejection. The Nusselt numbers measured for case 9 are compared directly with those obtained for case 5 (smooth trapezoidal channel); therefore, the resulting ratio is a clear indication of the heat transfer enhancement due to the V-shaped ribs in the wedge-shaped channel. The trend observed in this trapezoidal channel is similar to that of the rectangular channel, as the rib effect is isolated from the channel cross section. As with the rectangular ribbed duct, the center region experiences the greatest heat transfer enhancement. The middle region is followed by the inner and outer regions, which provide approximately the same level of heat transfer enhancement. The difference between the inner and outer regions is reduced when compared with the rectangular channel (Fig. 9). This is a result of the trapezoidal cross section. With the narrow channel, the secondary flow induced by the V-shaped ribs is not as clearly defined as within the rectangular channel. The structure of the counter-rotating vortices begins to break down, and additional mixing of the coolant pursues. The result is additional heat transfer enhancement on all surfaces within the channel. Although both the inner and outer surfaces provide approximately the same level of enhancement, it is interesting to observe in the latter half of the channel that the inner surface provides greater (albeit marginal) enhancement than the outer surface. The trailing-edge ejection tends to increase the heat transfer on the outer surface; however, the narrow cross section offers resistance to the coolant flow. With the V-shaped ribs inducing secondary flow toward both the inner and outer surfaces, the inner surface provides increased heat transfer coefficients. The smooth side wall sees the least heat transfer enhancement; however, the heat transfer coefficients are enhanced with the addition of ribs on the wide wall. Another difference between the rib-roughened wedge-shaped channel and the rib-roughened rectangular channel is the heat transfer enhancement in the streamwise direction. With case 3, the Nusselt number ratios in the rectangular channel gradually increase through the channel to $x/D_h = 7$, and near the end of the channel, the heat transfer coefficients begin to gradually decrease (this is most obvious along the outer and middle surfaces). Su et al. [26] confirmed this behavior through numerical prediction for a 4:1 channel. The predicted Nusselt number ratios increased from the inlet of the channel to a maximum value as the counter-rotating vortices, induced by the V-shaped ribs, gained strength. Beyond $x/D_h = 6$ the Nusselt number showed a very gradual decrease to the end of the channel ($x/D_h = 8$). The current trapezoidal channel shows the same trend (case 9). However, as the hydraulic diameter is reduced, when compared with the rectangular channel, the channel is nearly 16 hydraulic diameters long (compared with approximately 9 for the rectangular channel). The decrease in the heat transfer coefficients in the streamwise direction is more obvious for the wedge-shaped channel, which is relatively longer. However, the general trend of the heat transfer coefficients increasing to a maximum around $x/D_h = 7$ and then gradually decreasing remains valid.

The heat transfer enhancement due to ribs is also shown for the wedge-shaped channel with trailing-edge ejection in Fig. 11. The measured Nusselt numbers for case 10 are compared directly with case 6 to highlight the effect of the V-shaped rib turbulators. Unlike with the rectangular channel, the middle region experiences the greatest heat transfer enhancement, due to the turbulators, and the inner region closely follows. The Nusselt numbers on the outer surface in the smooth trapezoidal channel with ejection (case 6) are significantly higher than those on the other surfaces. The addition of ribs to the surface does not further enhance the already-high heat transfer coefficients. However, the ribs do increase the heat transfer

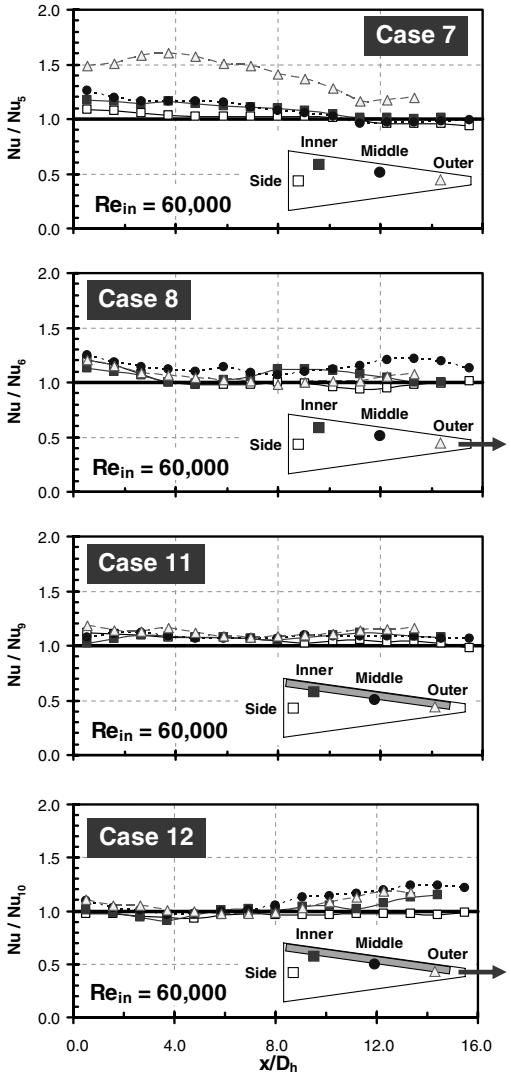

Fig. 12 Effect of entrance geometry on heat transfer enhancement in wedge-shaped channels (cases 7, 8, 11, and 12).

on the remaining surfaces that were adversely affected by the trailing-edge ejection. Heat transfer enhancement is observed on the side wall; however, this enhancement is only a fraction of that observed for the middle and inner surfaces (as these surfaces clearly benefit from the V-shaped ribs).

Finally, a more realistic model of a trailing-edge cooling passage is considered with the addition of a contraction into the heated portion of the test section. Figure 12 shows the heat transfer enhancement resulting from the contraction entrance. With case 7, the wedge-shaped channel is smooth and no coolant is extracted. The Nusselt numbers are compared directly with case 5, and so the effect of the entrance condition is isolated. For the one flow rate shown, the outer surface is most profoundly impacted by the entrance condition. As explained previously, this should be expected, as the contraction ratio in this region is approximately 8.5:1. The behavior of flow through a sharp entrance is observed, with the gradual increase of the outer surface heat transfer coefficients to a maximum and with the gradual decrease to a fully developed value. The slight increase is the result of the boundary-layer reattachment after the flow is forced through the contraction. The other three regions see slightly elevated heat transfer coefficients near the entrance of the channel, and they gradually decrease to a Nusselt number of unity. The effect of the entrance geometry is reduced when trailing-edge ejection is employed. As shown with case 8 (compared with case 6), the Nusselt number ratios are approximately 1.2 at the entrance of the channel, and they quickly reduce to unity along all surfaces. The heat transfer coefficients along the outer surface are elevated due to the ejection, and so the additional enhancement due to the entrance is minimal.

Within the rib-roughened trapezoidal passages, the effect of the entrance configuration is further reduced. As shown with the comparison of case 11 with case 9, the effect of the entrance condition is negligible. Similar trends were observed by Wright et al. [27] when they compared various entrance conditions in stationary and rotating ribbed channels. This trend is reinforced with the evaluation of the Nusselt number in the trapezoidal channel with ejection and a sharp entrance (case 12). The Nusselt number ratios deviate from unity near the end of the channel, where there is likely a variation in the flow rates between the two cases.

Figures 13 and 14 compare the smooth- and ribbed-channel Nusselt numbers, respectively, for all cases. The smooth-channel Nusselt numbers are shown for two locations in the rectangular and trapezoidal channels in Fig. 13. One point is selected near the entrance of the channel ($x/D_h \cong 3$), and a second point is selected in the fully developed region of the channel ($x/D_h \cong 7$). To make a fair comparison between each case, the data are presented with respect to the local Reynolds number. In addition, the Nusselt number predicted for fully developed turbulent flow is also shown. On the inner surface, near the entrance of the channel ($x/D_h \sim 3$), the Nusselt numbers for the rectangular channels are in agreement with the Dittus-Boelter/McAdams correlation. It is expected that the inner surface is the least effected by the trailing-edge ejection; moreover, near the entrance of the channel, the effect of ejection is minimal. As the flow becomes thermally developed through the channel, trailing-edge ejection has an increased impact on the Nusselt number, and even the inner surface is affected by the ejection (case 2 shows the greatest Nusselt numbers at $x/D_h \sim 7$ on the inner surface). Near the entrance of the channel, only the outer surface experiences a variation in the heat transfer coefficients from case to case, and as

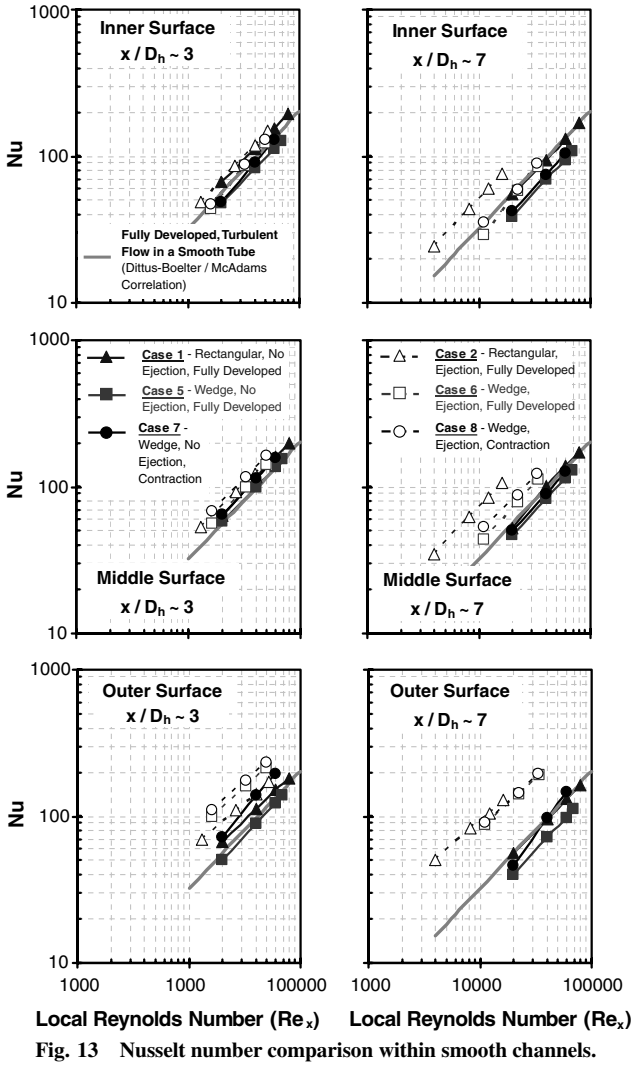

Fig. 13 Nusselt number comparison within smooth channels.

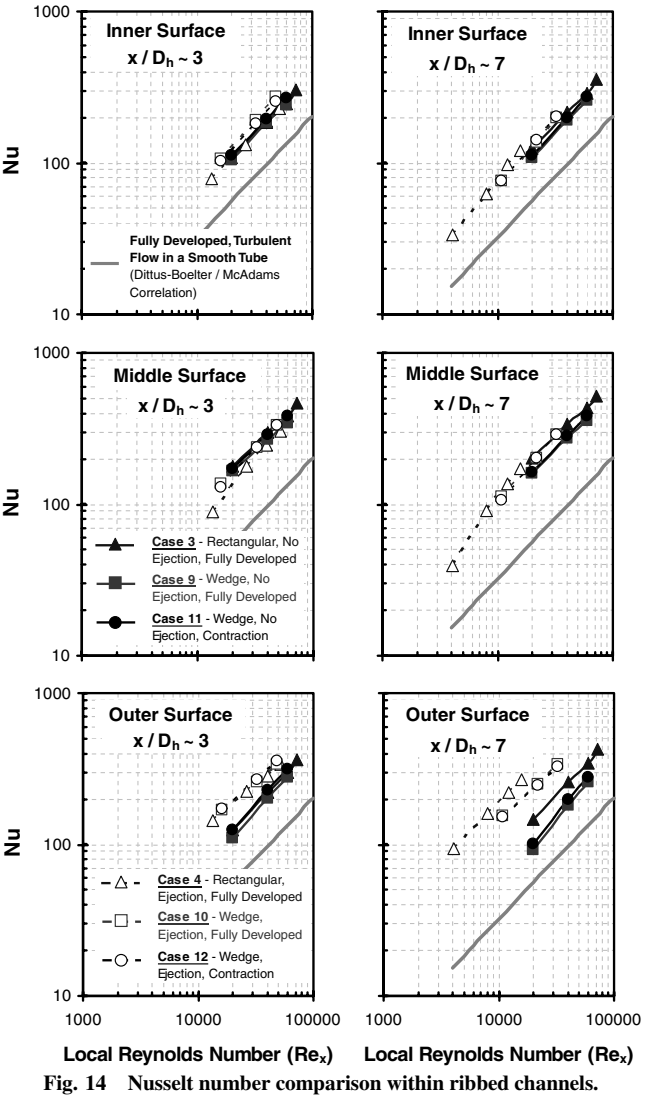

Fig. 14 Nusselt number comparison within ribbed channels.

expected, the wedge-shaped channel with the contraction entrance yields the greatest Nusselt numbers (case 8, outer surface, $x/D_h \sim 3$). Further downstream in the channel, there is a significant difference between the channels with ejection and those without. For both the middle and outer surfaces, the greatest heat transfer enhancement is observed in cases 2, 6, and 8. As the flow moves in the spanwise direction through the ejection slots, heat transfer enhancement results. The level of enhancement on the middle surface varies depending on the cross section of the channel (and corresponding ejection slot geometry).

The Nusselt numbers for the ribbed surfaces at two distinct locations are shown in Fig. 14. The heat transfer enhancement due to the ribs is greatest in the center of the channel, and this is reflected by the relatively high Nusselt numbers for the middle surface. As expected, all surfaces yield increased heat transfer when compared with the corresponding smooth channels. However, it is interesting to note that the effect of trailing-edge ejection is significantly reduced when compared with the smooth channels. Although the effect is reduced, the largest variation among the cases remains on the outer surface: most notably, far downstream ($x/D_h \sim 7$). With the V-shaped rib configuration used in this study, the rib-induced secondary flow is away from the center of the channel. Therefore, near the heated surface, the coolant naturally travels from the center of the channel toward the ejection slots. The addition of the ejection slots does not significantly alter the flow structure and the result is less variation from the channels with ejection than those without. If a different rib configuration were chosen, a different result would be expected, as the interaction of the rib-induced flow must be considered in conjunction with the ejection flow.

Conclusions

This experimental investigation has studied heat transfer enhancement in various cooling channels that model passages that are typical of those located near the trailing edges of turbine blades and vanes. The effects of channel cross section, surface roughness, coolant extraction, and entrance condition have been considered. The Nusselt numbers in the rectangular channel are adequately predicted by the traditional Dittus-Boelter/McAdams correlation; however, this correlation overpredicts the Nusselt numbers observed in the wedge-shaped channel (without ejection). In both rectangular and wedge-shaped channels, the Nusselt numbers decrease in the presence of trailing-edge ejection. However, this effect is not global, as the heat transfer coefficients increase along the outer surface (which is adjacent to the ejection slots). When V-shaped ribs are placed on the surface, the center of the rectangular channel experiences the greatest heat transfer enhancement, due to the secondary flow along the ribs. However, when V-shaped ribs are coupled with trailing-edge ejection, both the middle surface and the outer surface experience heat transfer enhancement (combined effect of rib configuration and coolant extraction). The effect of entrance geometry is most clearly seen in the smooth trapezoidal channel without ejection. In the most realistic configuration, composed of a wedge-shaped channel with both V-shaped ribs and coolant extraction, the effect of the entrance condition is marginal.

This experimental investigation has attempted to isolate several variables that might be encountered in trailing-edge cooling passages of gas turbine blades. However, the study has been limited to only two cross sections. In addition, only rib geometry has been considered. Finally, the effect of trailing-edge ejection has been considered by requiring 100% of the coolant flow to exit the channel through the trailing-edge slots. To gain a complete picture of trailing-edge cooling, it is necessary to consider a variety of trailing-edge channel shapes and sizes with varying rib configurations. Finally, including the effect of the coolant ejection with tip flow to eliminate the potential dead spot at the end of the channel should be considered.

References

[1] Han, J. C., Dutta, S., and Ekkad, S. V., *Gas Turbine Heat Transfer and Cooling Technology*, Taylor and Francis, New York, p. 646, 2000.

[2] Han, J. C., "Heat Transfer and Friction Characteristics in Rectangular Channels with Rib Turbulators," *Journal of Heat Transfer*, Vol. 110, No. 2, 1988, pp. 321–328.

[3] Han, J. C., and Park, J. S., "Developing Heat Transfer in Rectangular Channels with Rib Turbulators," *International Journal of Heat and Mass Transfer*, Vol. 31, No. 1, 1988, pp. 183–195. doi:10.1016/0017-9310(88)90235-9

[4] Park, J. S., Han, J. C., Huang, Y., Ou, S., and Boyle, R. J., "Heat Transfer Performance Comparisons of Five Different Rectangular Channels with Parallel Angled Ribs," *International Journal of Heat and Mass Transfer*, Vol. 35, No. 11, 1992, pp. 2891–2903. doi:10.1016/0017-9310(92)90309-G

[5] Han, J. C., Zhang, Y. M., and Lee, C. P., "Augmented Heat Transfer in Square Channels with Parallel, Crossed, and V-Shaped Angled Ribs," *Journal of Heat Transfer*, Vol. 113, No. 3, Aug. 1991, pp. 590–596. doi:10.1115/1.2910606

[6] Lau, S. C., Kukreja, R. T., and McMillin, R. D., "Effects of V-Shaped Rib Arrays on Turbulent Heat Transfer and Friction of Fully Developed Flow in a Square Channel," *International Journal of Heat and Mass Transfer*, Vol. 34, No. 7, 1991, pp. 1605–1616. doi:10.1016/0017-9310(91)90140-A

[7] Han, J. C., and Zhang, Y. M., "High Performance Heat Transfer Ducts with Parallel Broken and V-shaped Broken Ribs," *International Journal of Heat and Mass Transfer*, Vol. 35, No. 2, 1992, pp. 513–523. doi:10.1016/0017-9310(92)90286-2

[8] Taslim, M. E., Li, T., and Kercher, D. M., "Experimental Heat Transfer and Friction in Channels Roughened with Angled, V-Shaped, and Discrete Ribs on Two Opposite Walls," *Journal of Turbomachinery*, Vol. 118, No. 1, Jan. 1996, pp. 20–28.

[9] Ekkad, S. V., and Han, J. C., "Detailed heat Transfer Distribution in Two-Pass Square Channels with Rib Turbulators," *International Journal of Heat and Mass Transfer*, Vol. 40, No. 11, 1997, pp. 2525–2537. doi:10.1016/S0017-9310(96)00318-3

[10] Cho, H. H., Wu, S. J., and Kwon, H. J., "Local Heat/Mass Transfer Measurements in a Rectangular Duct with Discrete Ribs," *Journal of Turbomachinery*, Vol. 122, No. 3, July 2000, pp. 579–586. doi:10.1115/1.1303049

[11] Gao, X., and Suden, B., "Heat Transfer and Pressure Drop Measurements in Rib-Roughened Rectangular Ducts," *Experimental Thermal and Fluid Science*, Vol. 24, Mar. 2001, pp. 25–34. doi:10.1016/S0894-1777(00)00054-6

[12] Rhee, D. H., Lee, D. H, Cho, H. H., and Moon, H. K., "Effects of the duct Aspect Ratios on Heat /Mass Transfer with Discrete V-Shaped Ribs," American Society of Mechanical Engineers Paper GT2003-38622, 2003.

[13] Lowdermilk, W. H., Weiland, W. F., and Livingood, J. N. B., "Measurement of Heat Transfer and Friction Coefficients for Flow of Air in Noncircular Ducts at High Surface Temperatures," NACA RM E53J07, 1954.

[14] Ahn, S. W., and Son, K. P., "Heat Transfer and Pressure Drop in the Roughened Equilateral Triangular Duct," *International Communications in Heat and Mass Transfer*, Vol. 29, No. 4, May 2002, pp. 479–488. doi:10.1016/S0735-1933(02)00345-7.

[15] Obot, N. T., "Heat Transfer in a Smooth Scalene Triangular Duct with Two Rounded Corners," *International Communications in Heat and Mass Transfer*, Vol. 12, No. 3, May–June 1985, pp. 251–258. doi:10.1016/0735-1933(85)90048-X

[16] Zhang, Y. M., Gu, W. Z., and Han, J. C., "Augmented Heat Transfer in Triangular Ducts with Full and Partial Ribbed Walls," *Journal of Thermophysics and Heat Transfer*, Vol. 8, No. 3, July–Sept. 1994, pp. 574–579. doi:10.2514/3.580

[17] Eckert, E. R. G., and Irvine, T. F., "Pressure Drop and Heat Transfer in a Duct with Triangular Cross Section," *Journal of Heat Transfer*, Vol. 82, May 1960, pp. 125–138.

[18] Lau, S. C., Han, J. C., and Kim, Y. S., "Turbulent Heat Transfer and Friction in Pin Fin Channels with Lateral Flow Ejection," *Journal of Heat Transfer*, Vol. 111, No. 1, Feb. 1989, pp. 51–58.

[19] Lau, S. C., Han, J. C., and Batten, T., "Heat Transfer, Pressure Drop, and Mass Flow Rate in Pin Fin Channels with Long and Sort Trailing Edge Ejection Holes," *Journal of Turbomachinery*, Vol. 111, No. 2, Apr. 1989, pp. 116–123.

[20] Kumaran, T. K., Han, J. C., and Lau, S. C., "Augmented Heat Transfer in a Pin Fin Channel with Short or Long Ejection Holes," *International Journal of Heat and Mass Transfer*, Vol. 34, No. 10, Oct. 1991, pp. 2617–2628. doi:10.1016/0017-9310(91)90101-J

[21] Taslim, M. E., Li, T., and Spring, S. D., "Experimental Study of the

Effects of Bleed Holes on Heat Transfer and Pressure Drop in Trapezoidal Passages with Tapered Turbulators," *Journal of Turbomachinery*, Vol. 117, No. 2, Apr. 1995, pp. 281–289.

[22] Hwang, J. J., and Lu, C. C., "Lateral-Flow Effect on Endwall Heat Transfer and Pressure Drop in a Pin Fin Trapezoidal Duct with Various Pin Shapes," *Journal of Turbomachinery*, Vol. 123, No. 1, Jan. 2001, pp. 133–139. doi:10.1115/1.1333093

[23] Kline, S. J., and McClintock, F. A., "Describing Uncertainties in Single-Sample Experiments," *Mechanical Engineering*, Vol. 75, No. 1, 1953, pp. 3–8.

[24] Rohsenow, W. M., and Choi, H., *Heat, Mass, and Momentum Transfer*, Prentice–Hall, Upper Saddle River, NJ, 1961, pp. 192–193.

[25] Wright, L. M., Fu, W. L., and Han, J. C., "Thermal Performance of Angled, V-Shaped, and W-Shaped Rib Turbulators in Rotating Rectangular Cooling Channels ($AR = 4{:}1$)," *Journal of Turbomachinery*, Vol. 126, No. 4, 2004, pp. 604–614. doi:10.1115/1.1791286

[26] Su, G., Teng, S., Chen, H. C., and Han, J. C., "Computation of Flow and Heat Transfer in Rotating Rectangular Channels ($AR = 4$) with V-Shaped Ribs by a Reynolds Stress Turbulence Model," American Society of Mechanical Engineers Paper GT2003-38348, 2003.

[27] Wright, L. M., Lee, E., and Han, J. C., "Influence of Entrance Geometry on Heat Transfer in Rotating Rectangular Cooling Channels ($AR = 4{:}1$) with Angled Ribs," *Journal of Heat Transfer*, Vol. 127, No. 4, 2005, pp. 378–387. doi:10.1115/1.1860564